GAAL, S., BERG, K., TRANELL, G., OLSEN, S. and TANGSTAD, M. An investigation into aspects of liquid phase reduction of maganese and silica containing slag. *VII International Conference on Molten Slags Fluxes and Salts,* The South African Institute of Mining and Metallurgy, 2004.

An investigation into aspects of liquid phase reduction of maganese and silica containing slag

S. GAAL*, K. BERG*, G. TRANELL†, S.E. OLSEN* AND M. TANGSTAD‡

**Faculty of Science and Technology, NTNU, Trondheim, Norway*

†SINTEF Materials Technology, Trondheim, Norway

‡Eramet Research Norway, Trondheim, Norway

In this study, the reduction behaviours of MnO and SiO_2 containing slags by solid carbonaceous materials was investigated in both small and larger-scale laboratory experiments. Five types of carbonaceous material were investigated: 2 graphites, industrial coke, anthracite and eucalyptus charcoal. The effects of the reductant type/properties on the reduction kinetics, metal composition and metal yield, have been quantified. Results show that the reduction rate is highly dependant on the type of carbon used. It was found that the reductant type significantly influenced the SiO_2 reduction while it did not seem to have a large effect on the MnO reduction. This may be due to the different CO_2 and SiO reactivities of the materials.

Introduction

High carbon ferromanganese alloy is produced by reducing manganese ores with carbon. This process results in a bi-product of about 600—700 kg of liquid slag per ton of alloy. This slag consists mainly of MnO (30–50%) and SiO_2 (20–30%), and is a valuable commercial product that is normally used as a raw material for production of high silicon ferromanganese alloys. The present study was initiated with the purpose of providing more knowledge and fundamental understanding of the mechanisms of MnO and SiO_2 reduction from liquid manganese silicate slags by solid carbonaceous reductants.

The reduction of MnO/SiO_2 from slag is a complex process to study experimentally due to the number of phases involved and the dynamic reduction behaviour at the reaction interfaces. The overall silicon and manganese transfer reactions can be expressed as:

$$(MnO) + C \quad \underline{Mn} + CO(g) \qquad [1]$$

$$(SiO_2) + 2C \quad \underline{Si} + 2CO(g) \qquad [2]$$

where brackets denote slag constituents and underlining denotes the metal phase solution. The thermodynamics for these reactions is well described in the literature, so that for a given slag composition, amount of slag, temperature and carbon activity, the expected yield of manganese and silicon metal at complete equilibrium may be calculated.

Although MnO is reduced by both solid and solute carbon, SiO_2 can only be reduced by solute carbon or solid carbon in the presence of metallic Fe or Mn (because the formation of Si metal requires a low Si activity). The transfer reaction of manganese from slag to metal, reaction [1], has been investigated at temperatures up to 1550ºC[1-4], using graphite crucibles as the reductant and slags with an MnO content of up to 70%. It seems that the MnO reduction kinetics is intrinsically controlled, with an activation energy of about 370 kJ/mol.

In a system with simultaneous reduction of MnO and SiO_2, the slag/metal exchange reaction of manganese and silicon, which is a combination of [1] and [2], has to be taken into account:

$$2(MnO) + \underline{Si} \quad \underline{2Mn} + (SiO_2) \qquad [3]$$

This reversible reaction is usually considered to be faster than the carbothermic reactions [1] and [2]. Hence, partial slag/metal equilibrium may be established between manganese and silicon. If so, the kinetics of reactions [1] and [2] will be mutually linked through reaction [3] and the overall reduction rates thus limited by the slower carbothermic reduction reaction.

While the manganese and silicon transfers may be expressed through reactions [1], [2] and [3], the actual routes through which the reduction of MnO and SiO_2 take place are more complex. It is reasonably well established in the literature[5-7] that the reduction path from SiO_2 in slag to Si in metal largely involves the formation and reduction of SiO gas through reactions [4] and [5].

$$(SiO_2) + CO(g) \rightarrow SiO(g) + CO_2(g) \qquad [4]$$

$$SiO(g) + \underline{C} \rightarrow \underline{Si} + CO(g) \qquad [5]$$

It has been proposed[6] for Fe-Si that reduction occurs primarily at the slag/gas and gas/metal interfaces inside bubbles attached to the carbonaceous material, because bubble nucleation would be thermodynamically favourable there. The equilibrium partial pressures of SiO and CO_2 in reaction [4] are extremely small. At 1600ºC, the maximum

product of the partial pressures of SiO and CO_2 can be calculated as 2.0×10^{-6} x α_{SiO_2} atm^2 (where α_{SiO_2} is the silica activity). The driving force and kinetics for reaction [5] will be determined by the SiO pressure generated from reaction [4], and this is again dependent upon the CO_2 pressure at the slag/gas interface. This CO_2 pressure may be controlled either by the rate at which CO_2 is transported away from the interface or by the rate at which CO_2 reacts with C and forms CO. If the conditions for a low CO_2 pressure are better facilitated at the slag/metal/carbon three phase zone, then this could explain the (possibly) faster reaction rates there. Thus, it is possible that the reaction of CO_2 with carbon has a big influence on the kinetics of silica reduction.

A mechanism for MnO reduction by carbon has not been proposed, but it has been found[7] that the reduction rate of ferromanganese slags by solid carbon is very dependent on the gas composition, and proposed that the kinetics is controlled by both the intrinsic reaction and mass transfer limitations in the gas phase. Drawing a parallel to FeO reduction, there seems to be consensus in the literature that FeO reduction from slags by carbon takes places via the reduction of FeO by CO gas to Fe metal and CO_2 at the slag/gas interface, followed by the regeneration of CO via the Boudouard reaction at the slag/metal interface. It is possible that the same mechanism applies to MnO reduction. Thus, it is possible that the reaction of CO_2 with carbon has a big influence on the kinetics of MnO reduction, similar to the SiO_2 reduction.

There are of course a number of factors that influence the behaviour of this reaction system, such as temperature, slag composition, gas composition etc. The present work, however, focuses mainly on how the properties of the carbonaceous material may influence the reaction kinetics and metal yield.

Experimental procedures

As the main focus of the study involved the role of reductant type/properties on the slag reduction, a part of the study was dedicated to characterization of the physical and chemical properties of the carbonaceous materials used. Characterization parameters and methods are described below.

In order to obtain a comprehensive picture of the reduction behaviour of slags containing manganese oxides and silica, kinetic information was gathered through two different experimental approaches, as described below.

Characterization of reductant materials

Five different solid carbonaceous materials were used in various parts of the study. These materials were: two types of commercial graphites, Siberian Anthracite, 'industrial coke' (blast furnace coke, commonly used in the production of Mn based alloy products) and eucalyptus charcoal (produced in Brazil). The physical and chemical properties determined for these materials are described below.

Fixed carbon

The quantity of carbon remaining after removing the volatiles and moisture by heating, less the remaining ash.

Porosity

Porosity related parameters, such as pore area per unit weight, average/median pore diameters based on volume and area, skeletal density, and porosity, were determined through mercury porosimetry, performed by the Particle & Surface Sciences Applications Laboratory in Gosford, Australia. It is generally acknowledged that the pore volumes determined via this method are larger than if measured by, for example, the nitrogen adsorption method. This is due to the fact that porosimetry includes more pore volume data in the macro pore region[8].

Ash

It has recently been noted[9] that the reaction rate between solid carbon and liquid slag may be affected by the composition (and potentially mineralogy) of the ash present in the carbonaceous material. Hence, the five different carbonaceous materials were ashed at 600ºC, and their ash contents determined. Compositions of these ashes were determined through X-ray Fluorescence (XRF).

Sulphur content

Sulphur is a strongly surface active element and has previously been shown to have an accelerating effect on slag reduction when present in the slag[3]. If present in the carbonaceous material (as organic or inorganic sulphur), it may influence the slag reduction rate. The sulphur contents of the carbonaceous materials were determined by LECO combustion analysis.

Ordered carbonaceous material characteristics

The characteristics of ordered carbonaceous materials are generally determined through XRD. Fine powdered material (-106μm) was dispersed with acetone on a glass slide sample holder. The sample was scanned at a wavelength of 1.54056 Å, with a step size of 0.02º, at 0.5s/step. From the X-ray spectra, structural parameters such as d (carbon layer spacing) and L_c (the thickness of the carbon layer stack) were determined. d was determined through Bragg's law:

$$d = \frac{\lambda}{2\sin\theta} \qquad [6]$$

where λ is the wavelength of the X-ray employed and θ is the position (reflection angle) of the main (002) peak. L_c can be calculated using the Scherrer Equation[10],

$$L_e = \frac{0.89\lambda}{B\cos\theta} \qquad [7]$$

where 0.89 is a constant given by the reflection plane, λ is the wavelength of the X-ray employed, B is the angular (2θ) width (rad) at a half maximum intensity of the main peak (002), and θ is the position (reflection angle) of the main peak (002).

The X-ray spectra can also give an indication of the relative fractions ordered vs. amorphous carbonaceous material. Numerous methods for estimation of the fraction amorphous material has been suggested in the literature. In this study, the fraction amorphous material was estimated from a simple ratio of the diffuse portion of the spectra to the total[10].

CO_2 reactivity

CO_2 reactivity is a parameter frequently used for the characterization of reductants in various metallurgical processes. CO_2 reactivity describes the propensity of a carbonaceous material to react with CO_2 gas at a given temperature and is further described as follows.

Table I
Composition of slag used for the small kinetic experiments, after melting and solidifying

	Industrial (%)
MnO	45.6
SiO_2	22.9
CaO	13.9
Al_2O_3	10.5
MgO	4.6
K_2O	1.3
Na_2O	-
BaO	0.8
FeO	0.07
S	0.3
Fe metal	1.9
Mn metal	~ 6

Several mechanisms have been proposed for the C-CO_2 reaction. Ergun's[11] proposed, and widely used, mechanism is described as:

$$C_f + CO_2 \underset{k_1}{\overset{k_1}{\leftrightarrow}} C(O) + CO \quad [8]$$

$$C(O) \underset{k_2}{\rightarrow} CO + C_f \quad [9]$$

Equation [8] represents an oxygen exchange reaction where carbon dioxide dissociates at an active site on the carbon surface (C_f), releasing a molecule of carbon monoxide and forming a carbon-oxygen surface complex ($C(O)$). Equation [9] represents the dissociation of the carbon-oxygen surface complex from the carbon surface, forming carbon monoxide. Given the importance of the CO_2 partial pressure in the gas for the SiO_2 reduction described in the introduction (and potentially for the MnO reduction), the relative CO_2 reactivity of the carbonaceous materials was determined.

The reaction rate between the carbon and the carbon dioxide is affected by:

- Concentration of active sites on the carbon surface
- Accessibility of internal surface area to reacting gas
- Catalytic material present

In this study, the CO_2 reactivity for the five carbonaceous materials was measured at 1000ºC in a 100% CO_2 atmosphere. The reactivity measurements were carried out in a TGA where an initial 0.5 grams of material was heated in argon to 1000ºC and held until no weight loss was recorded. At this point the furnace atmosphere was replaced with CO_2. The conversion rate was subsequently calculated at 35% conversion of the available fixed carbon.

Small-scale kinetic reduction experiments

A small resistance furnace with a vertical graphite tube heating element was used for the reduction experiments. Cylindrical graphite crucibles of 40 mm i.d. and 50 mm deep were used as both the sample container and reductant, and were charged with 50g of slag. The two different graphite materials, here referred to as 'G1' and 'G2' were used for the crucibles. The experiments were carried out at 1600ºC and 1 atm CO, with a constant CO flow rate set to 0.2 Nl/min. Several experiments of different duration (with subsequent quenching) were required in order to obtain a complete reduction course for MnO and SiO_2, but monitoring the amount of off-gas provided a rough indicator of the kinetics during a single experiment. The following data was collected for each experiment:

- Composition of the slag after each experiment, determined by microprobe
- Weight of the sample before and after the experiment
- Weight of the metal after the experiment (separating the phases is difficult and hence not very accurate. Nevertheless, an estimate was provided)
- Volume of off-gas
- Silicon content of the metal, determined by ICP analysis

The total amounts of MnO and SiO_2 reduced were calculated from mass balances with respect to Al_2O_3 in the slag, since this had proven to be the most reliable calculation method in previous work[1-4]. The (very small) amount of FeO reduced to Fe metal was also calculated in this way. The amount of Si metal formed was determined from the Si analysis and the weight of the metal. By comparing this with the overall SiO_2 reduction from the slag, the Si yield could be calculated. The Mn yield could be estimated by calculating the amount of Mn in the metal and comparing this with the overall MnO reduction. (The Fe content was assumed constant, while the carbon content was estimated from solubility data.)

An industrial ferromanganese slag was used for the kinetic experiments. The compositions of the slag was determined by electron microprobe analysis of a 50 g sample that had been melted in a graphite crucible and cooled immediately upon melting (solidifying took 1–2 minutes). Ferromanganese slags always contain some ferromanganese metal. A wet chemical analysis of the finely crushed slag/metal mixture showed that the total Fe content (as FeO in the slag and Fe in metal) was 1.95% by weight. The Mn metal content was estimated by assuming that the Mn:Fe ratio in the metal phase was similar to that of industrial ferromanganese alloys. The composition of the slag is given in Table I.

Larger-scale laboratory experiments

Larger experiments were also performed in an induction furnace to investigate the reduction behaviour of three different carbonaceous materials, other than graphite. A graphite crucible 80 mm inside diameter was used to contain 500 g of industrial ferromanganese slag, which was heated to 1600ºC and held for 20 minutes. In the first experiment the extent of reduction by the graphite was determined, which was then compared to experiments with the addition of 100 g of coke, anthracite or charcoal (+10–15mm). The content of the crucible was stirred every 5 minutes with a graphite rod. After the allotted time period, the contents of the crucible were quenched in a graphite mould, and the reactants were separated, weighed and analysed. The 'external' surface area of the different types of carbon was measured optically using a digital camera to determine the perimeter of the particles, which was then used to calculate the external surface area.

Results

Properties of carbonaceous reductants

The physical and chemical properties determined for the carbonaceous reductants are summarized in Tables II and III.

As seen from Table II, while the overall porosity of the carbonaceous materials, with the exception of anthracite, does not seem to vary significantly, their pore sizes do. It can also be noted that the coke has moderately large crystalline carbon regions while the anthracite, and especially the eucalyptus charcoal, have far more amorphous carbon present. Naturally, the two graphites display very crystalline structures. Graphite I is, however,

Table II
Summary of physical and chemical properties of carbonaceous materials used in the study

Property (unit)	G1	G2	Anthracite	Industrial Coke	Eucalyptus Charcoal
Fix C (%)	99.87	99.62	94.3	89.36	81.3
Ash (wt%)	0.13	0.38	2.8	10.64	0.43
VM (wt%)	-	-	3.0	-	18.3
Porosity (%)	23.5	25.5	4.9	27.5	27.3
Average pore diameter (μm)	0.05	0.03	0.02	0.57	0.46
Median pore dia. (area)* (μm)	0.012	0.009	0.009	0.008	0.019
Median pore dia. (vol)**(μm)	1.8	0.6	0.03	26.8	12.4
Total pore area (m^2/g)	11.70	18.80	6.34	1.86	3.86
Skeletal density (g/ml)	2.20	2.17	1.62	1.45	0.90
d (Å)	3.4	3.4	3.5	3.5	3.8
Lc (Å)	260.5	215.3	14.2	23.4	11.5
Approx. fraction amorphous C	***	***	0.42	0.18	0.69
S content (ppm)	42	35	2600	5600	20
CO_2 react. (s^{-1})	$1.3x10^{-4}$	$5.4x10^{-5}$	$3.17x10^{-5}$	$2.78x10^{-5}$	$7.23x10^{-4}$

*pore diameter of pores contributing 50% of the pore area
**pore diameter of pores contributing 50% of the pore volume
***negligible

notably more crystalline than graphite II. As far as measured physical and chemical properties go, the CO_2 reactivity of the different materials, expressed as the conversion rate at 35% conversion, may only be correlated to the median pore diameter with respect to pore area, as seen in Figure 1.

It can also been seen from Tables II and III that while the overall sulphur content of the charcoal is very low, it is concentrated in the ash, indicating that essentially all sulphur in the charcoal is inorganic/mineral-bound sulphur. In both the anthracite and the coke, it appears that the concentration of sulphur in the ash compared to overall concentration is not significantly larger, indicating that while the ash contains sulphur, most of the sulphur is present as organic sulphur.

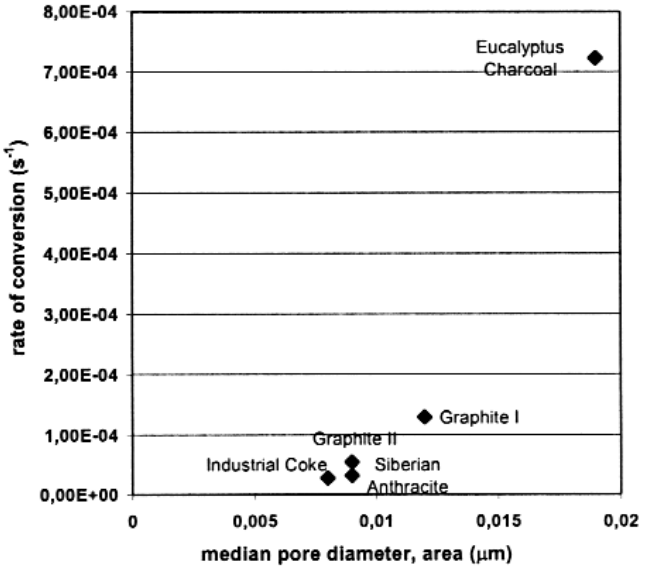

Figure 1. Rate of carbon conversion as function of median pore diameter (by pore area)

Results of small-scale kinetic experiments

The MnO, SiO_2 and Al_2O_3 contents of the industrial slag after various times of reduction, for the two different types of graphite, are given in Table IV.

The calculated reduction versus time relationships for MnO in the industrial slag, using the two different graphites as reductant, are illustrated in Figure 2.

It is seen that the slag composition changes very little during the last hour with G1 as reductant, indicating that equilibrium is reached, while with G2 the reduction has not

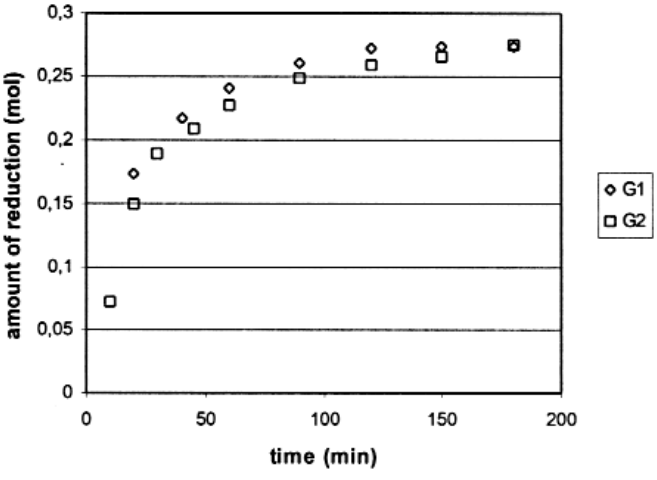

Figure 2. Effect of graphite type on MnO reduction

Table III
Chemical composition of ash in the carbonaceous materials

Ash comp.	Anthracite	Industrial coke	Eucalyptus charcoal
SiO_2	43.38	51.96	34.32
Al_2O_3	34.26	32.61	10.06
CaO	1.17	1.87	15.25
Fe_2O_3	6.18	4.99	2.06
SO_3	1.17	1.22	9.19
K_2O	1.76	1.16	6.80
Na_2O	0.60	0.69	4.32
MgO	1.32	0.78	4.52
P_2O_5	1.11	0.73	2.33
TiO_2	0.98	1.53	0.34

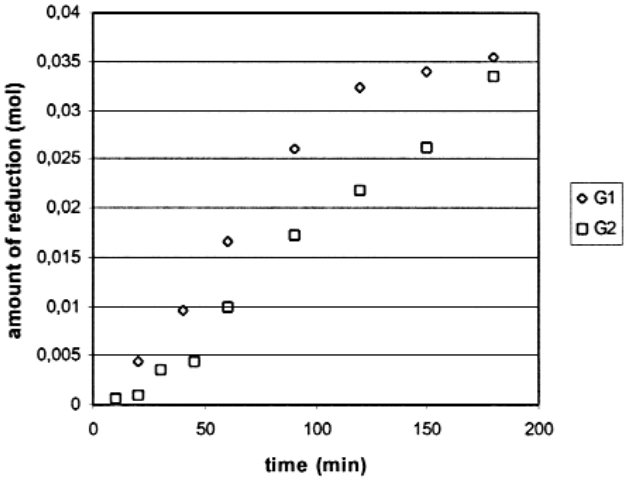

Figure 3. Effect of graphite type on overall SiO_2 reduction

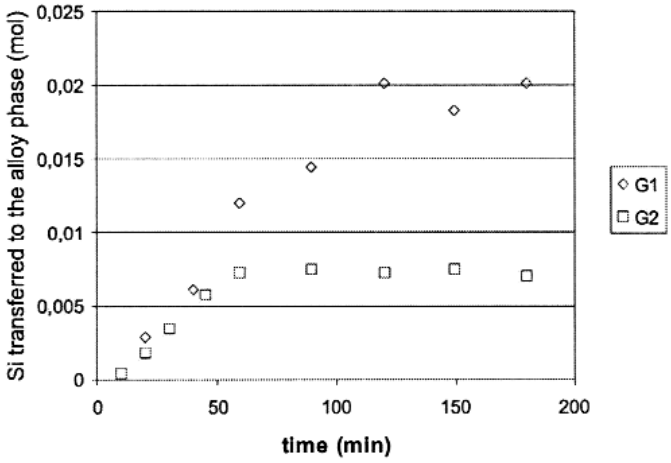

Figure 4. Effect of graphite type on amount of Si transferred to the alloy phase

reached completion after three hours. These differences are, however, too small to confidently conclude that the MnO reduction kinetics are different with the two materials G1 and G2.

The data for SiO_2 reduction, shown in Figure 3, indicate that there is a larger difference between the reductants G1 and G2, that is, the SiO_2 reduction rate is faster during the first two hours with G1 as reductant. After two hours, the reduction rate with G1 as reductant slows down considerably as equilibrium is approached, while in the case of G2 there is no such tendency during the final stages. It is interesting to notice also that the rate of silica reduction seems to be relatively constant, in accordance with most of the literature data on reduction of silica from slags by carbon in liquid iron (although the metal melt covered the bottom of the crucible in those investigations).

As mentioned, it was difficult to assess the Mn loss from the system. Most likely it was between 10 and 20% for both of the cases, but it was not possible to determine if/how the manganese loss would vary during the course of reduction. The distribution of Si between the metal and the gas phase, however, was readily calculated, and the results are given in Table V.

The SiO_2 reduction data was divided into Si metal and SiO gas formed as functions of time, as shown in Figures 4 and 5. The diagrams show that the main difference in reduction behaviour between the two systems is that with G1, the SiO_2 reduction takes place with an SiO loss of about 35–45% (increasing toward the end) until equilibrium is reached, while with G2 the SiO loss is less to begin with (25–30%), but becomes 100% after about an hour of reduction. Figure 4 indicates clearly that the rate of Si transfer to the metal is about equal for the two cases during the first hour, and that the rate is linear.

As was seen from the CO_2 reactivity measurements of the two graphites, G1 had a higher reactivity than G2 (and potentially higher SiO reactivity), which may explain the higher yield of Si to the metal phase with G1 as reductant in the initial stages of reduction.

Larger-scale laboratory experiments

The composition of the initial slag, final slag and metal are given in Table VI.

When the reduction behaviour of the three different types of carbon is compared to the experiment in the graphite crucible, it can be clearly seen that the reduction rate is increased. The quantity of metal produced, slag reduced and the concentration of silicon in the metal all indicate significant differences in the behaviour of the different reductants. The coke was the least reactive, while the anthracite and charcoal were similar, depending on the criteria used to compare them. Although the experiments were performed with a constant weight of carbon added, the surface area of carbon on contact with the slag varied due to the different shapes of particles used.

Table IV
Composition of industrial slag after different periods of reduction (%)

	G1			G2		
Time (min.)	MnO	SiO_2	Al_2O_3	MnO	SiO_2	Al_2O_3
0	45.8	22.9	10.2	45.6	22.9	10.5
10				39.5	25.7	11.8
20	27.9	30.9	14.1	30.4	29.4	13.5
30				25	31.7	14.8
40	21.1	33.3	15.7			
45				21.8	33.1	15.5
60	16.8	34.3	16.8	18.7	33.7	16.3
90	13	34.7	18	14.7	34.4	17.4
120	10.4	34.9	18.9	12.8	34.7	18.1
150	10.2	34.8	19	11.4	34.7	18.6
180	10	34.7	19.1	9.2	34.2	19.2

Table V
Distribution of Si between the metal and gas phase

	G1			G2		
Time (min.)	Metal wt (g)	Si (%)	SiO lost (%)	Metal wt (g)	Si (%)	SiO lost (%)
10				5.16	0.23	27.3
20	10.82	0.75	35.1	9.27	0.57	
30				11.79	0.84	
40	13.06	1.33	35.1			
45				13.00	1.25	
60	14.50	2.31	27.8	13.44	1.52	26.4
90	15.55	2.6	44.6	14.70	1.45	55.8
120	16.43	3.45	37.7	15.50	1.33	66.4
150	16.50	3.1	46.5	16.00	1.33	71.1
180	16.50	3.42	43.4	16.28	1.22	78.9

Table VI
Results for reduction of industrial slag by different types of carbon

	Initial	Graphite	Coke	Anthracite	Charcoal
Time (min)	0	20	20	20	20
Slag wt (g)	500	254.1	240.3	216	205.3
Metal wt (g)		129.8	138.1	168.3	173.1
Surface area (m^2/kg*)			0.473	0.552	1.52
SiO lost (g)		10.3	9.7	11.4	18.7
kg metal/h.m^2*			0.53	2.09	0.86
kg metal/h.kg*			0.25	1.16	1.30
kg metal/h.kg▫			0.28	1.22	2.36
Slag analysis					
Mn (%)	33.4	6	5.48	4.98	1.61
SiO_2 (%)	24.9	33.62	34.6	34.55	29.62
CaO (%)	13.1	26.39	26.25	26.29	30.68
K_2O (%)	1.5	0.22	0.4	0.46	0.05
TiO_2 (%)	0.5	0.52	0.45	0.5	0.23
BaO (%)	0.8	1.7	1.52	1.64	1.92
MgO (%)	9.8	9.13	9.04	9.03	10.68
Al_2O_3 (%)	12.2	19.64	19.72	19.72	23.06
FeO (%)	2.0	0.09	0.11	0.07	0.08
Metal analysis					
Mn (%)		82.9	82.0	79.3	81.6
Si (%)		3.3	4.7	4.6	8.7

* reductant, ▫fixed carbon
Note: surface area reported is the external surface area, not including porosity for the size carbon materials actually used in the experiments

Significantly, the experiments showed that the charcoal provided good reduction kinetics, reducing more of the slag than both coke and anthracite, while producing more metal per unit carbon—with a larger concentration of Si. This is illustrated in Figures 6 and 7. The concentration of MnO in the reduced slag was also lower with charcoal than with the other reductants.

Discussion and conclusions

As illustrated by the results above, the type of carbonaceous material used for the reduction of a typical industrial ferromanganese slag will affect the amount and composition of metal produced. Both small-scale experiments with different types of graphite and larger-scale experiments with 'industrial' reductants such as coke, anthracite and charcoal, showed that the reductant type seems to significantly influence the SiO_2 reduction while it did not seem to have a large effect on the MnO reduction. This may indicate that the MnO reduction is mainly affected by the availability of dissolved carbon (which seems to be similar/sufficient for all materials) and not limited by variations in CO_2 pressure, which is set by the CO_2 reactivity of the carbon materials. As for SiO_2 reduction, the small-scale experiments indicate that the SiO_2 reduction is faster with the more CO_2 reactive graphite (G1) than the less reactive. The reasons why G1 is more CO_2 reactive than G2 may be related to the pore area/pore volume distribution, as indicated by Figure 1. G1 also has a higher L_c value than G2. High L_c values are generally associated with higher rates of metal dissolution[12]. The larger scale experiments also show that more CO_2 reactive reductants give a higher metal yield with more SiO_2 reduced. The reactivity from highest to lowest of the three 'industrial' reductants was: eucalyptus charcoal, anthracite and industrial coke. In this case, the reactivity of the

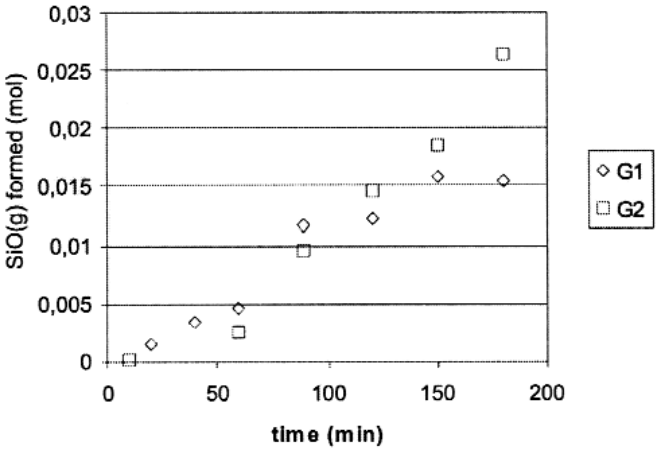

Figure 5. Effect of graphite type on the amount of SiO(g) formed

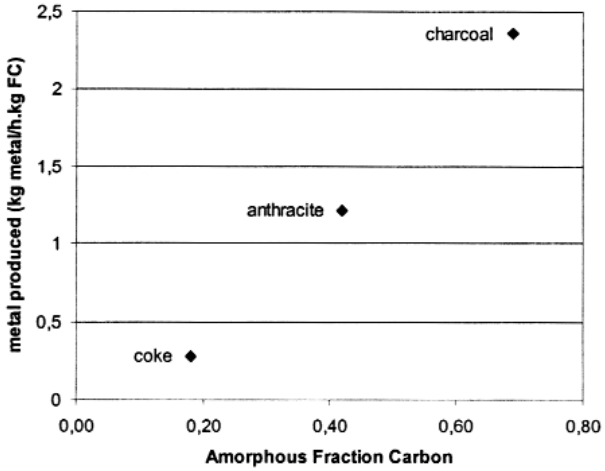

Figure 6. The effect of amorphous fraction of carbon on the amount of metal produced

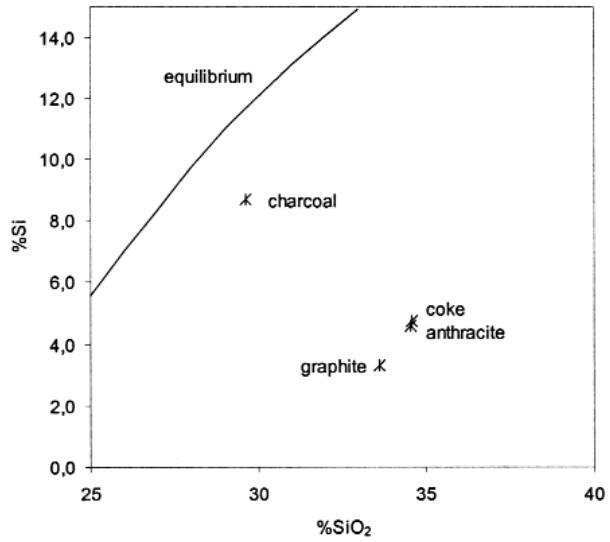

Figure 7. The influence of reductant type on the concentration of silicon in the metal as a function of silica in the slag for the present investigation

materials may have more to do with the fraction of amorphous carbon present in the material than their crystallite characteristics. An additional factor to the Si yield is the "SiO reactivity" of the materials. A significantly larger SiO reactivity is expected for the charcoal than for the coke[13].

Acknowledgements

The authors wish to acknowledge the project funds provided by the Norwegian Research Council and the Norwegian Ferro-alloy Producers Research Association, through the CarboMat programme.

References

1. OLSØ, V., TANGSTAD, M. and OLSEN, S.E. Reduction kinetics of MnO-saturated slags, *INFACON 8*, Beijing, China, 1998, pp. 279–283.
2. SKJERVHEIM, T.A. and OLSEN, S.E. The rate and mechanism for reduction of manganese oxide from silicate slags, *INFACON 7*, Trondheim, Norway, 1995, pp. 631–639.
3. SKJERVHEIM, T.A. Kinetics and mechanisms for transfer of manganese and silicon from molten oxide to liquid manganese metal, Dr.Ing. dissertation, NTH, Trondheim, Norway, MI-rapport 1994:26.
4. TANGSTAD, M. The high-carbon ferromanganese process – coke bed relations, Dr.Ing. dissertation, NTH, Trondheim, Norway, MI-rapport 1996:37.
5. POMFRET, R.J. and GRIEVESON, P. Kinetics of slag-metal reactions , *Can. Metall. Quart.*, vol. 22, no. 3, 1983, pp. 287–299.
6. TURKDOGAN, E.T., GRIEVESON, P. and BEISLER, J.F. Kinetic and equilibrium considerations for silicon reaction between silicate melts and graphite-saturated iron. Part II. Reaction kinetics of silica reduction, *Trans. Metall. Soc.* AIME, 227, 1963, pp. 1265–1274.
7. YASTREBOFF, M., OSTROVSKI, O. and GANGULY, S. Effect of gas composition on the carbothermic reduction of manganese oxide, *ISIJ Int.*, vol. 43, no.2 , 2003, pp. 161–165.
8. WHITE, W.E., BARTHOLOMEW, C.H., HECKER, W.C., SMITH, D.M. Changes in Surface Area, Ore Structure and Density during Formation of High Temperature Chars from Representative U.S. Coals, *Adsorption Sci. Technol.*, vol. 7, 1991, pp. 180–209.
9. MEHTA, A.S., SAHAJWALLA, V. Influence of Temperature on the Wettability at the Slag/Carbon Interface during Pulverised Coal Injection in a Blast Furnace, *Scand. J. Metallurg.*, vol. 30, 2001, pp. 370–378.
10. KLUG, H.P., ALEXANDER, L.E. *X-ray Diffraction Procedures for Polycrystalline and Amorphous Materials*, John Wiley & Sons, New York, 1974.
11. ERGUN, S.J. *Physical Chemistry*, vol. 60, 1956, p. 480.
12. WU, C., WIBLEN, R. and SAHAJWALLA; V Influence of Ash on Mass Transfer and Interfacial Reaction between Natural Graphite and Liquid Iron, *Met. Mat. Trans. B*, vol. 31B, 2000, pp. 1099–1104.
13. TUSET, J.K. and RAANESS, O. Reactivity of Reduction Materials for the Production of Silicon, Silicon-Rich Ferroalloys and Silicon Carbode, *Electric Furnace Proceedings*, 1976, pp. 101–107.